A derivation of three-dimensional ray equations in ellipsoidal coordinates

Jianguo Yan and Kang K. Yen
Department of Electrical and Computer Engineering, Florida International University, Miami, Florida 33199

(Received 30 September 1992; revised 27 July 1994; accepted 26 October 1994)

Conventional three-dimensional (3-D) ray equations ignore the effect of Earth flattening, whereas this effect, as has been shown by Munk *et al.* [J. Phys. Oceanogr. **18**, 1876–1898 (1988)], cannot be ignored for long-range transmissions. To take into account the earth flattening, new 3-D ray equations are derived, in this paper, in terms of the ellipsoidal coordinates: Geographic latitude, longitude, and depth. The new 3-D equations account for both Earth curvature and Earth flattening, and thus are more accurate than those conventional 3-D ray equations. It is shown that under certain circumstances, the new equations reduce to the horizontal ray equations of Munk *et al.*, the Aki-Richards 3-D spherical ray equations, and the conventional two-dimensional ray equations, respectively. The advantages of using the new equations in ocean acoustics are discussed. Numerical examples are presented.

PACS numbers: 43.30.Cq

INTRODUCTION

Recently, there has been a growing interest in long-range, low-frequency acoustic propagation in the ocean. Often, ray tracing is performed for studying this problem. Although in this case ray theory might not strictly apply, the ray paths constructed still provide a first look at the acoustic waves.

For studying long-range wave propagation, three-dimensional (3-D) Hamiltonian ray equations formulated by Jones *et al.*[1] have been used by many investigators[2–6] in ocean acoustics. There is another set of 3-D ray equations, Aki–Richards equations,[7] which are usually employed in seismology. Both equations are written in spherical coordinates, so that they do not take into account the effect of Earth flattening, whereas this effect, as has been shown by Munk *et al.*,[8] cannot be ignored for long-range transmissions.

Assuming that the Earth is an ellipsoid, Munk *et al.*[8] have derived a set of horizontal ray equations. The equations are written in the coordinates: ϕ, λ, and α (geographic latitude, longitude, and azimuth), which are consistent with those in Geodesy. They used the equations to construct the ray paths from Perth, Australia to Bermuda and concluded that "for long-range transmissions we cannot ignore Earth flattening." Since in Geodesy the Earth's departure from a sphere is known to be too great and ellipsoid is considered as a good approximation to the Earth,[9] the horizontal ray equations of Munk *et al.* are obviously better equations for studying long-range acoustic propagation in the ocean. Heaney *et al.*[10] have presented a more general derivation of the horizontal ray equations. Their[10] adiabatic mode approach clears up some of the unresolved questions raised in Ref. 8.

The horizontal ray equations are very useful for solving long-range problems. However, they deal with only horizontal or two-dimensional (2-D) problem in latitude–longitude plane. Many applications in ocean acoustics require modeling acoustic fields for 3-D environments. To take into account Earth flattening in 3-D ray equations, Dworski and Mercer[11] have adapted the Hamiltonian ray equations formulated by Jones *et al.*[1] for spherical coordinates to the ellipsoidal coordinates (colatitude, longitude, and geocentrical radius to the ray point). But, as they stated in the report, "one problem related to data representation remains... These are, as stated, geocentrical equations on the ellipsoid, but they are not oblate spheroidal equations. For them, even a level sea surface, or a flat bottom, has a radial position that varies with the horizontal coordinates."[11]

We have derived a set of 3-D ray equations in the ellipsoidal coordinates (geographic latitude, longitude, and ocean depth). Because the coordinates we used are consistent with those in Geodesy,[9,12] we do not have the problem of data representation mentioned by Dworski and Mercer.[11] We have not seen any published reference to the equations we derived, and therefore, present the derivation of the equations in this paper. In the first section, we give a description about the ellipsoidal, geographic coordinates. The derivation of the ray equations is presented in the second section. We show, in the third section, that under certain circumstances our 3-D equations reduce to Munk *et al.*'s equations, Aki–Richards 3-D equations, and conventional 2-D ray equations, respectively. We also discuss the advantages of using our equations in ocean acoustics. Numerical examples are presented in the last section.

I. COORDINATES

Let us assume that the Earth is an ellipsoid and consider the ellipsoidal coordinates (ϕ,λ,r) shown in Fig. 1, where ϕ is geographic latitude, north positive, λ is longitude, east of Greenwich being positive, and r is ocean depth, downward positive. Then the Cartesian coordinates (x,y,z) of any point in the Earth can be expressed as

 0001-4966/95/97(3)/1538/7/$6.00

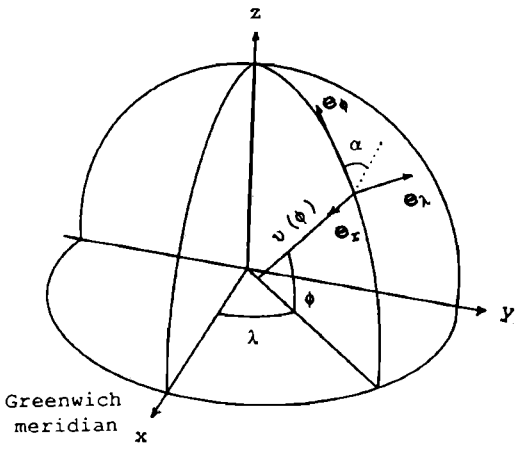

FIG. 1. Coordinates. Orthogonal unit vectors $(\mathbf{e}_\phi,\mathbf{e}_\lambda,\mathbf{e}_r)$ in (ϕ,λ,r) directions of the ellipsoidal coordinates; ϕ is geographic latitude, north positive, λ is longitude, east of Greenwich being positive, and r is ocean depth, downward positive. v is the radius of curvature in prime vertical. Dashed line is the projection of a local ray path onto the $\phi\lambda$ plane. α, azimuth, is the angle between $\mathbf{e}_\phi$ and the projection of the ray path onto the $\phi\lambda$ plane.

$$x=(v-r)\cos\phi\cos\lambda,$$
$$y=(v-r)\cos\phi\sin\lambda, \tag{1}$$
$$z=[(1-e^2)v-r]\sin\phi,$$

where e is the eccentricity of the ellipsoid, and v is the radius of curvature in prime vertical, expressed as[12]

$$v=a/(1-e^2\sin^2\phi)^{1/2}. \tag{2}$$

Here, a is the semimajor radius of the reference ellipsoid. If the depth r vanishes, Eqs. (1)–(3) will reduce to those in Geodesy, e.g., Eq. (A.51) in Ref. 12, the distinction being our use of depth as an additional dimension. We call the coordinates (ϕ,λ,r) ellipsoidal coordinates, because they are based on the reference ellipsoid in Fig. 1.

Let

$$\mathbf{R}=x\mathbf{e}_x+y\mathbf{e}_y+z\mathbf{e}_z \tag{3}$$

be a position vector, where $\mathbf{e}_x$, $\mathbf{e}_y$, and $\mathbf{e}_z$ are the unit vectors in the directions of increasing x, y, and z, respectively, then the unit tangent vector in the ϕ direction is

$$\mathbf{e}_\phi=\frac{\partial\mathbf{R}/\partial\phi}{h_\phi}, \tag{4}$$

where

$$h_\phi=\left|\frac{\partial\mathbf{R}}{\partial\phi}\right|. \tag{5}$$

Similarly, the unit tangent vectors in the directions of λ and r are

$$\mathbf{e}_\lambda=\frac{\partial\mathbf{R}/\partial\lambda}{h_\lambda} \tag{6}$$

and

$$\mathbf{e}_r=\frac{\partial\mathbf{R}/\partial r}{h_r}, \tag{7}$$

where

$$h_\lambda=\left|\frac{\partial\mathbf{R}}{\partial\lambda}\right| \tag{8}$$

and

$$h_r=\left|\frac{\partial\mathbf{R}}{\partial r}\right|. \tag{9}$$

The quantities h_ϕ, h_λ, and h_r are scale factors. The unit vectors $\mathbf{e}_\phi$, $\mathbf{e}_\lambda$, and $\mathbf{e}_r$ are in the directions of increasing ϕ, λ, and r, respectively.

From Eqs. (1) and (3), we have

$$\begin{aligned}\frac{\partial\mathbf{R}}{\partial\phi}&=\frac{\partial x}{\partial\phi}\mathbf{e}_x+\frac{\partial y}{\partial\phi}\mathbf{e}_y+\frac{\partial z}{\partial\phi}\mathbf{e}_z\\&=\left(\frac{\partial v}{\partial\phi}\cos\phi-(v-r)\sin\phi\right)\\&\quad\times(\cos\lambda\mathbf{e}_x+\sin\lambda\mathbf{e}_y)+\Big((1-e^2)\\&\quad\times\frac{\partial v}{\partial\phi}\sin\phi+[(1-e^2)v-r]\cos\phi\Big)\mathbf{e}_z.\end{aligned} \tag{10}$$

Considering Eq. (2), we rewrite Eq. (10) as

$$\begin{aligned}\frac{\partial\mathbf{R}}{\partial\phi}&=-\sin\phi(\mu-r)(\cos\lambda\mathbf{e}_x+\sin\lambda\mathbf{e}_y)\\&\quad+\cos\phi(\mu-r)\mathbf{e}_z,\end{aligned} \tag{11}$$

where

$$\mu=a(1-e^2)/(1-e^2\sin^2\phi)^{3/2} \tag{12}$$

is the radius of curvature.[12]

From Eqs. (5) and (11) the scale factor in the ϕ direction is written as

$$h_\phi=\mu-r. \tag{13}$$

Substituting Eqs. (11) and (13) into (4) gives

$$\mathbf{e}_\phi=-\sin\phi(\cos\lambda\mathbf{e}_x+\sin\lambda\mathbf{e}_y)+\cos\phi\mathbf{e}_z. \tag{14}$$

Similarly, using Eqs. (1), (3), (6)–(9), we obtain the other two unit vectors:

$$\mathbf{e}_\lambda=-\sin\lambda\mathbf{e}_x+\cos\lambda\mathbf{e}_y \tag{15}$$

and

$$\mathbf{e}_r=-\cos\phi(\cos\lambda\mathbf{e}_x+\sin\lambda\mathbf{e}_y)-\sin\phi\mathbf{e}_z \tag{16}$$

with the corresponding scale factors:

$$h_\lambda=(v-r)\cos\phi \tag{17}$$

and

$$h_r=1. \tag{18}$$

We have obtained the unit tangent vectors and corresponding scale factors for the ellipsoidal coordinates shown in Fig. 1. It is easy to show that $\mathbf{e}_\phi\times\mathbf{e}_\lambda=\mathbf{e}_r$, i.e., the unit vectors are orthogonal.

II. DERIVATION OF RAY EQUATIONS

Using the position vector $\mathbf{R}$, we can write the unit vector along a local ray path as

$$\sigma=\frac{d\mathbf{R}}{ds}=\frac{\partial\mathbf{R}}{\partial\phi}\frac{d\phi}{ds}+\frac{\partial\mathbf{R}}{\partial\lambda}\frac{d\lambda}{ds}+\frac{\partial\mathbf{R}}{\partial r}\frac{dr}{ds}$$
$$=h_\phi\dot{\phi}\mathbf{e}_\phi+h_\lambda\dot{\lambda}\mathbf{e}_\lambda+h_r\dot{r}\mathbf{e}_r, \tag{19}$$

where s is path length and

$$(\dot{\ })=\frac{d}{ds}. \tag{20}$$

Equations (4), (6), and (7) were used in deriving Eq. (19).

We can also write the unit vector along a local ray path in a different way. Let us define the direction of a ray path by two angles α and θ: θ is the angle between the ray direction and the $\phi\lambda$ plane; α is the angle between $\mathbf{e}_\phi$ and the projection of the ray path onto the $\phi\lambda$ plane. Then we can write

$$\sigma=\cos\theta\cos\alpha\mathbf{e}_\phi+\cos\theta\sin\alpha\mathbf{e}_\lambda+\sin\theta\mathbf{e}_r. \tag{21}$$

Comparing Eq. (19) with (21) and using (13), (17), and (18) we have

$$\dot{\phi}=\cos\theta\cos\alpha/(\mu-r) \tag{22}$$

$$\dot{\lambda}=\cos\theta\sin\alpha/[(\upsilon-r)\cos\phi] \tag{23}$$

and

$$\dot{r}=\sin\theta. \tag{24}$$

Now we have three differential equations with five unknown variables ϕ, λ, r, α, and θ. To construct the ray path, we still need two additional equations for α and θ. We derive the two additional equations as follows.

Taking the derivative of Eq. (21) with respect to path length, we obtain

$$\dot{\sigma}=-\sin\theta\dot{\theta}(\cos\alpha\mathbf{e}_\phi+\sin\alpha\mathbf{e}_\lambda)+\sin\theta\dot{\mathbf{e}}_r+\cos\theta$$
$$\times(-\sin\alpha\dot{\alpha}\mathbf{e}_\phi+\cos\alpha\dot{\mathbf{e}}_\phi+\cos\alpha\dot{\alpha}\mathbf{e}_\lambda+\sin\alpha\dot{\mathbf{e}}_\lambda$$
$$+\theta\dot{\mathbf{e}}_r). \tag{25}$$

Using Eqs. (14)–(16), we write

$$\dot{\mathbf{e}}_\phi=\dot{\phi}\mathbf{e}_r-\sin\phi\dot{\lambda}\mathbf{e}_\lambda, \tag{26}$$

$$\dot{\mathbf{e}}_\lambda=\dot{\lambda}(\sin\phi\mathbf{e}_\phi+\cos\phi\mathbf{e}_r), \tag{27}$$

and

$$\dot{\mathbf{e}}_r=-\dot{\phi}\mathbf{e}_\phi-\cos\phi\dot{\lambda}\mathbf{e}_\lambda. \tag{28}$$

Substituting Eqs. (26)–(28) into (25) gives

$$\dot{\sigma}=\mathbf{e}_\phi[-\sin\theta(\dot{\theta}\cos\alpha+\dot{\phi})+\cos\theta\sin\alpha(\dot{\lambda}\sin\phi$$
$$-\dot{\alpha})]+\mathbf{e}_\lambda[-\sin\theta(\dot{\theta}\sin\alpha+\dot{\lambda}\cos\phi)$$
$$+\cos\theta\cos\alpha(\dot{\alpha}-\dot{\lambda}\sin\phi)]+\mathbf{e}_r[\cos\theta(\cos\alpha\dot{\phi}$$
$$+\sin\alpha\cos\phi\dot{\lambda}+\dot{\theta})]. \tag{29}$$

Through Eq. (29), $[\cos\alpha(\mathbf{e}_\lambda\cdot\dot{\sigma})-\sin\alpha(\mathbf{e}_\phi\cdot\dot{\sigma})]$ yields

$$\dot{\alpha}=[\cos\theta\sin\phi\dot{\lambda}+\sin\theta(\cos\alpha\cos\phi\dot{\lambda}-\sin\alpha\dot{\phi})$$
$$+\cos\alpha(\mathbf{e}_\lambda\cdot\dot{\sigma})-\sin\alpha(\mathbf{e}_\phi\cdot\dot{\sigma})]/\cos\theta \tag{30}$$

and $\{\sin\theta[\sin\alpha(\mathbf{e}_\lambda\cdot\dot{\sigma})+\cos\alpha(\mathbf{e}_\phi\cdot\dot{\sigma})]-\cos\theta(\mathbf{e}_r\cdot\dot{\sigma})\}$ gives

$$\dot{\theta}=-\sin\alpha\cos\phi\dot{\lambda}-\cos\alpha\dot{\phi}-\sin\theta[\sin\alpha(\mathbf{e}_\lambda\cdot\dot{\sigma})$$
$$+\cos\alpha(\mathbf{e}_\phi\cdot\dot{\sigma})]+\cos\theta(\mathbf{e}_r\cdot\dot{\sigma}). \tag{31}$$

In Eqs. (30) and (31), $\dot{\phi}$, $\dot{\lambda}$, and $\dot{r}$ can be replaced by Eqs. (22)–(24), but we still need to formulate the derivative of σ. This can be done by using Fermat's principle.

The travel time of an eigenray is

$$t=\int N(\phi,\lambda,r)[(ds\ \sigma)\cdot(ds\ \sigma)]^{1/2}$$
$$=\int N(\phi,\lambda,r)(\sigma\cdot\sigma)^{1/2}ds=\int L(\phi,\lambda,r,\dot{\phi},\dot{\lambda},\dot{r})ds, \tag{32}$$

where

$$N(\phi,\lambda,r)=1/C(\phi,\lambda,r). \tag{33}$$

Here C denotes sound speed as a function of position. Fermat's principle states that the path a ray will take is such that the travel time will be an extremum. Therefore, according to calculus of variations, we have

$$\frac{\partial L}{\partial\phi}-\frac{d}{ds}\left(\frac{\partial L}{\partial\dot{\phi}}\right)=0, \tag{34}$$

$$\frac{\partial L}{\partial\lambda}-\frac{d}{ds}\left(\frac{\partial L}{\partial\dot{\lambda}}\right)=0, \tag{35}$$

$$\frac{\partial L}{\partial r}-\frac{d}{ds}\left(\frac{\partial L}{\partial\dot{r}}\right)=0, \tag{36}$$

where L is Lagrangian. Using Eq. (32) we write

$$\frac{\partial L}{\partial\phi}=\frac{\partial N}{\partial\phi}(\sigma\cdot\sigma)^{1/2}+\frac{1}{2}N2\sigma\cdot\frac{\partial\sigma}{\partial\phi}\Big/(\sigma\cdot\sigma)^{1/2}$$
$$=\frac{\partial N}{\partial\phi}+N\sigma\cdot\left(\frac{\partial\sigma}{\partial\phi}\right). \tag{37}$$

Similarly, we write

$$\frac{\partial L}{\partial\lambda}=\frac{\partial N}{\partial\lambda}+N\sigma\cdot\left(\frac{\partial\sigma}{\partial\lambda}\right), \tag{38}$$

$$\frac{\partial L}{\partial r}=\frac{\partial N}{\partial r}+N\sigma\cdot\left(\frac{\partial\sigma}{\partial r}\right), \tag{39}$$

$$\frac{\partial L}{\partial\dot{\phi}}=N\sigma\cdot\left(\frac{\partial\sigma}{\partial\dot{\phi}}\right), \tag{40}$$

$$\frac{\partial L}{\partial\dot{\lambda}}=N\sigma\cdot\left(\frac{\partial\sigma}{\partial\dot{\lambda}}\right), \tag{41}$$

and

$$\frac{\partial L}{\partial\dot{r}}=N\sigma\cdot\left(\frac{\partial\sigma}{\partial\dot{r}}\right). \tag{42}$$

Substituting Eqs. (37) and (40) into (34) gives

$$\frac{\partial N}{\partial \phi}+N\sigma\cdot\frac{\partial \sigma}{\partial \phi}-\left[\left(\dot{\phi}\frac{\partial N}{\partial \phi}+\dot{\lambda}\frac{\partial N}{\partial \lambda}+\dot{r}\frac{\partial N}{\partial r}\right)\sigma\cdot\left(\frac{\partial \sigma}{\partial \dot{\phi}}\right)+N\left(\dot{\sigma}\cdot\left(\frac{\partial \sigma}{\partial \dot{\phi}}\right)+\sigma\cdot\frac{d}{ds}\left(\frac{\partial \sigma}{\partial \dot{\phi}}\right)\right)\right]=0. \tag{43}$$

Similarly, substituting Eqs. (38) and (41) into (35) results in

$$\frac{\partial N}{\partial \lambda}+N\sigma\cdot\left(\frac{\partial \sigma}{\partial \lambda}\right)-\left[\left(\dot{\phi}\frac{\partial N}{\partial \phi}+\dot{\lambda}\frac{\partial N}{\partial \lambda}+\dot{r}\frac{\partial N}{\partial r}\right)\sigma\cdot\left(\frac{\partial \sigma}{\partial \dot{\lambda}}\right)+N\left(\dot{\sigma}\cdot\left(\frac{\partial \sigma}{\partial \dot{\lambda}}\right)+\sigma\cdot\frac{d}{ds}\left(\frac{\partial \sigma}{\partial \dot{\lambda}}\right)\right)\right]=0. \tag{44}$$

By using Eqs. (39) and (42), Eq. (36) can be rewritten as

$$\frac{\partial N}{\partial r}+N\sigma\cdot\left(\frac{\partial \sigma}{\partial r}\right)-\left[\left(\dot{\phi}\frac{\partial N}{\partial \phi}+\dot{\lambda}\frac{\partial N}{\partial \lambda}+\dot{r}\frac{\partial N}{\partial r}\right)\sigma\cdot\left(\frac{\partial \sigma}{\partial \dot{r}}\right)+N\left(\dot{\sigma}\cdot\left(\frac{\partial \sigma}{\partial \dot{r}}\right)+\sigma\cdot\frac{d}{ds}\left(\frac{\partial \sigma}{\partial \dot{r}}\right)\right)\right]=0. \tag{45}$$

Using Eqs. (43)–(45), we write

$$\left(\frac{\partial N}{\partial \phi}+\frac{\partial N}{\partial \lambda}+\frac{\partial N}{\partial r}\right)+N\sigma\cdot\left(\frac{\partial \sigma}{\partial \phi}+\frac{\partial \sigma}{\partial \lambda}+\frac{\partial \sigma}{\partial r}\right)-\left(\frac{\dot{\phi}\partial N}{\partial \phi}+\dot{\lambda}\frac{\partial N}{\partial \lambda}+\dot{r}\frac{\partial N}{\partial r}\right)\sigma\cdot\left(\frac{\partial \sigma}{\partial \dot{\phi}}+\frac{\partial \sigma}{\partial \dot{\lambda}}+\frac{\partial \sigma}{\partial \dot{r}}\right)-N\dot{\sigma}\cdot\left(\frac{\partial \sigma}{\partial \dot{\phi}}+\frac{\partial \sigma}{\partial \dot{\lambda}}+\frac{\partial \sigma}{\partial \dot{r}}\right)-N\sigma\cdot\frac{d}{ds}\left(\frac{\partial \sigma}{\partial \dot{\phi}}+\frac{\partial \sigma}{\partial \dot{\lambda}}+\frac{\partial \sigma}{\partial \dot{r}}\right)=0. \tag{46}$$

As shown in the Appendix, the second term and the last term in Eq. (46) vanish. Therefore, Eq. (46) becomes

$$\left(\frac{\partial N}{\partial \phi}+\frac{\partial N}{\partial \lambda}+\frac{\partial N}{\partial r}\right)-\left(\dot{\phi}\frac{\partial N}{\partial \phi}+\dot{\lambda}\frac{\partial N}{\partial \lambda}+\dot{r}\frac{\partial N}{\partial r}\right)\sigma\cdot\left(\frac{\partial \sigma}{\partial \dot{\phi}}+\frac{\partial \sigma}{\partial \dot{\lambda}}+\frac{\partial \sigma}{\partial \dot{r}}\right)-N\dot{\sigma}\cdot\left(\frac{\partial \sigma}{\partial \dot{\phi}}+\frac{\partial \sigma}{\partial \dot{\lambda}}+\frac{\partial \sigma}{\partial \dot{r}}\right)=0. \tag{47}$$

Since the curvilinear coordinates (ϕ,λ,r) are orthogonal, we can write the gradient as[13]

$$\nabla=\frac{\mathbf{e}_\phi}{h_\phi}\frac{\partial}{\partial \phi}+\frac{\mathbf{e}_\lambda}{h_\lambda}\frac{\partial}{\partial \lambda}+\frac{\mathbf{e}_r}{h_r}\frac{\partial}{\partial r}. \tag{48}$$

Using Eq. (48) and multiplying Eq. (47) by $(\mathbf{e}_\phi/h_\phi+\mathbf{e}_\lambda/h_\lambda+\mathbf{e}_r/h_r)\cdot$, we obtain

$$\dot{\sigma}=\nabla\ln N-\sigma\sigma\cdot\nabla\ln N=(1-\sigma\sigma\cdot)\nabla\ln N. \tag{49}$$

From Eqs. (14) and (49), we have

$$\mathbf{e}_\phi\cdot\dot{\sigma}=\frac{1}{h_\phi}\frac{\partial}{\partial \phi}\ln N-\cos\theta\cos\alpha\left(\frac{\cos\theta\cos\alpha}{h_\phi}\frac{\partial}{\partial \phi}+\frac{\cos\theta\sin\alpha}{h_\lambda}\frac{\partial}{\partial \lambda}+\frac{\sin\theta}{h_r}\frac{\partial}{\partial r}\right)\ln N. \tag{50}$$

Similarly, using Eqs. (15), (16), and (49), we write

$$\mathbf{e}_\lambda\cdot\dot{\sigma}=\frac{1}{h_\lambda}\frac{\partial}{\partial \lambda}\ln N-\cos\theta\sin\alpha\left(\frac{\cos\theta\cos\alpha}{h_\phi}\frac{\partial}{\partial \phi}+\frac{\cos\theta\sin\alpha}{h_\lambda}\frac{\partial}{\partial \lambda}+\frac{\sin\theta}{h_r}\frac{\partial}{\partial r}\right)\ln N \tag{51}$$

and

$$\mathbf{e}_r\cdot\dot{\sigma}=\frac{1}{h_r}\frac{\partial}{\partial r}\ln N-\sin\theta\left(\frac{\cos\theta\cos\alpha}{h_\phi}\frac{\partial}{\partial \phi}+\frac{\cos\theta\sin\alpha}{h_\lambda}\frac{\partial}{\partial \lambda}+\frac{\sin\theta}{h_r}\frac{\partial}{\partial r}\right)\ln N. \tag{52}$$

Substituting Eqs. (50) and (51) into (30) and using Eqs. (13), (17), (22), and (23), we write

$$\dot{\alpha}=\frac{\cos\theta\tan\phi\sin\alpha}{v-r}+\sin\theta\sin\alpha\times\cos\alpha\left(\frac{1}{v-r}-\frac{1}{\mu-r}\right)+\left(-\frac{\sin\alpha}{\mu-r}\frac{\partial}{\partial \phi}+\frac{\cos\alpha}{(v-r)\cos\phi}\frac{\partial}{\partial \lambda}\right)\frac{\ln N}{\cos\theta}. \tag{53}$$

Similarly, substituting Eqs. (50)–(52) into (31) and using Eqs. (13), (17), (18), (22), and (23), we obtain

$$\dot{\theta}=-\cos\theta\left(\frac{\sin^2\alpha}{v-r}+\frac{\cos^2\alpha}{\mu-r}\right)+\left(-\frac{\sin\theta\cos\alpha}{\mu-r}\frac{\partial}{\partial \phi}-\frac{\sin\theta\sin\alpha}{(v-r)\cos\phi}\frac{\partial}{\partial \lambda}+\cos\theta\frac{\partial}{\partial r}\right)\ln N. \tag{54}$$

III. DISCUSSIONS

We have derived a set of 3-D ray equations in terms of the ellipsoidal coordinates. They are Eqs. (22)–(24), (53) and (54). These equations account for both Earth curvature and earth flattening, so that they are very useful for studying long-range acoustic propagation in the ocean.

The horizontal ray equations of Munk *et al.*[8] can be obtained as a special case of the 3-D equations derived in this paper. Setting θ (the angle between ray direction and the $\phi\lambda$ plane) to be zero and restricting $r=0$ force a ray to lie on the surface of the earth. Then Eqs. (22)–(24), (53), and (54) reduce to

$$\dot{\phi}=\cos\alpha/\mu, \tag{55}$$

$$\dot{\lambda}=\sin\alpha/(v\cos\phi), \tag{56}$$

and

$$\dot{\alpha}=\frac{\tan\phi\sin\alpha}{v}+\left(-\frac{\sin\alpha}{\mu}\frac{\partial}{\partial \phi}+\frac{\cos\alpha}{v\cos\phi}\frac{\partial}{\partial \lambda}\right)\ln N. \tag{57}$$

These are the horizontal ray equations, given by Heaney *et al.*[10] and equivalent to those used by Munk *et al.*[8]

Moreover, we will show that if ellipticity is neglected, our 3-D equations will reduce to the Aki–Richards 3-D spherical ray equations. Let us consider the spherical coordinates (Θ,Φ,R) used by Aki and Richards,[7] where Θ is co-latitude, Φ is longitude, and R is the distance from the center of the Earth. Then for the spherical Earth, we have

$$v=\mu=R_c \tag{58}$$

and we also have $R=R_c-r$, $\Theta=\pi/2-\phi$, $\Phi=\lambda$, $i=\pi/2+\theta$, and $\zeta=\pi-\alpha$, where R_c is the radius of spherical Earth, definitions of i and ζ are given in Ref. 7. Using these relations, our Eqs. (22)–(24), (53), and (54) reduce to

$$\dot{\Theta}=\sin i \cos\zeta/R \tag{59}$$

$$\dot{\Phi}=\sin i \sin\zeta/(R\sin\Theta) \tag{60}$$

$$\dot{R}=\cos i \tag{61}$$

$$\dot{\zeta}=-\frac{\sin\zeta}{R\sin i}\frac{1}{N}\frac{\partial N}{\partial\Theta}+\frac{\cos\zeta}{\sin i}\frac{1}{R\sin\Theta}\frac{1}{N}\frac{\partial N}{\partial\Phi}-\frac{1}{R}\sin i\sin\zeta\cot\Theta \tag{62}$$

and

$$\dot{i}=-\sin i\left(\frac{1}{R}+\frac{1}{N}\frac{\partial N}{\partial r}\right)+\frac{\cos i}{R}\left(\cos\zeta\frac{1}{N}\frac{\partial N}{\partial\Theta}+\frac{\sin\zeta}{\sin\Theta}\frac{1}{N}\frac{\partial N}{\partial\Phi}\right). \tag{63}$$

These are the Aki-Richards equations in Ref. 7.

We also note that if horizontal refractions and the effect of earth curvature are neglected (this implies that N depends only on the ocean depth r, $v\to\infty$, and $\mu\to\infty$), our Eqs. (22)–(24), (53), and (54) will reduce to the conventional 2-D ray equations:

$$\dot{r}=\sin\theta \tag{64}$$

and

$$\dot{\theta}=\frac{\cos\theta}{N}\frac{dN}{dr}, \tag{65}$$

which are identical to Eqs. (5.1.55) and (5.1.58) in the Ref. 14.

We have shown that under certain circumstances, our 3-D ray equations reduce to Munk *et al.*'s horizontal ray equations, Aki–Richards 3-D spherical ray equations, and conventional 2-D ray equations, respectively. This partially demonstrates the correctness of our 3-D ray equations. Using our 3-D equations has the following advantages:

(1) They do not have range limitation, while spherical ray equations may not be accurate enough for studying global-scale transmissions, and 2-D equations are valid for at most 100 km.

(2) They are convenient equations for source localization, because they use geographically measurable coordinates.

(3) Sound speed, rather than phase velocity, can be used directly for ray tracing. This allows us to avoid the influence of phase-velocity error on the determination of ray paths. The phase-velocity error may result from the perturbation of frequency, the correctness of ocean-bottom model and the errors of the geoacoustic data used in the ocean-bottom model. We believe that the horizontal ray equations[8,10] and the adiabatic mode approach,[10,15] which uses phase velocity for ray tracing, are very useful in studying long-range transmissions. The new 3-D ray equations, however, presents an alternative method.

IV. NUMERICAL EXAMPLE

For a numerical example, we consider the sound-speed model that has been used by Georges *et al.*[16] and Mercer *et al.*[17] The 3-D sound speed is expressed as

$$C(\phi,\lambda,r)=c(\phi,r)[1+E\exp(-D_\phi^2/W_\phi^2-D_\lambda^2/W_\lambda^2-D_r^2/W_r^2)]^{1/2}, \tag{66}$$

where

$$D_\phi=(\phi-\phi_0)/R_c, \tag{67}$$

$$D_\lambda=(\lambda-\lambda_0)/R_c, \tag{68}$$

$$D_r=r-r_0, \tag{69}$$

ϕ_0, λ_0, and r_0 are the latitude, longitude, and depth of the central maximum of the perturbation, respectively, W_ϕ, W_λ, and W_r are the Gaussian widths of the perturbation in the coordinate directions, E is a constant corresponding to the strength of the perturbation, and R_c is a constant corresponding to the radius of a spherical earth. The linearly zonal canonical sound speed is

$$c(\phi,r)=c_s(r)+K(\phi-\phi_s), \tag{70}$$

where ϕ_s is the latitude of the source, $c_s(r)$ is the canonical profile at the source, and K is the zonal gradient, expressed as

$$K=[c_R(r)-c_s(r)]/(\phi_R-\phi_s). \tag{71}$$

Here $c_R(r)$ and ϕ_R are the canonical profile and the latitude at the receiver, respectively. The canonical sound speed expression[18] is

$$c(r)=c_a\{1+\epsilon[\eta+\exp(-\eta)-1]\}, \tag{72}$$

where

$$\eta=2(r-r_a)/B, \tag{73}$$

c_a and r_a are the sound speed and the depth at channel axis, respectively, B is scale depth, and ϵ is perturbation coefficient.

In the following calculations, the acoustic source is located at 30°N, 100°E, and at a depth of 1 km. The receiver is placed at a depth of 1 km, and located at 38°59′N (0.68048613 rad), 100°E. The model parameters used here are $R_c=6374$ km, $\phi_0=\phi_s+500/R_c$, $\lambda_0=1.757095804$ rad,[19] $r_0=0.8$ km, $W_\phi=W_\lambda=150$ km, $W_r=1.2$ km, and $E=0.01345752$, which is correlated with 10 m/s central maximum perturbation.[19] At the source, c_a is 1.495 km/s, r_a is 1.2 km, B is 1.2 km, and ϵ is 0.005. At the receiver, c_a is

TABLE I. Effects of Earth flattening on 3-D eigenray's launch grazing and launch azimuthal angles, and travel times.

Eigenray identifier	Difference between spherical and ellipsoidal ray trace[a]		
	Grazing angle (deg)	Azimuth (deg)	Travel time (s)
33	0.076	0.001	1.868
34	0.083	0.000	1.871
35	0.094	−0.001	1.878
36	0.108	−0.002	1.880
37	0.132	−0.001	1.885
38	0.187	−0.003	1.890
−38	−0.172	−0.002	1.889
−37	−0.134	−0.002	1.883
−36	−0.107	0.000	1.877
−35	−0.091	0.000	1.873
−34	−0.082	0.000	1.873

[a]The difference was obtained by subtracting ellipsoidal ray parameters from spherical.

1.485 km/s, r_a is 0.9 km, B is 1.0 km, and ϵ is 0.0057. Fischer's reference ellipsoid[9] ($a=6378.150$ km, and $e=0.08181333$) is used.

Ray Eqs. (22)–(24), (53), and (54) were integrated by using the fourth-order Runge–Kutta method with adaptive stepsize control.[20] A ray was determined as an eigenray, if it passed within 2 m in depth, 0.5×10^{-6} rad in latitude and longitude of the receiver. With the same model parameters, we also performed spherical ray tracing using the Aki–Richards Eqs. (59)–(63), and compared the results with those of ellipsoidal ray tracing. In the spherical ray-tracing results, R was replaced by depth r ($R=R_c-r$), and i replaced by grazing angle θ ($i=\pi/2+\theta$).

Table I provides a comparison between ellipsoidal and spherical eigenrays. In this table, the eigenray identifier signifies the total number of ray-path turnovers and turnunders between the source and the receiver, and its sign indicates whether the ray left the source at an angle above (−) or below (+) the horizontal. We can see from this table that neglecting ellipticity produced travel time errors as large as 1.9 s. In the ellipsoidal earth case, the distance between the source and the receiver was 997.2 km, while it was 1000 km in the spherical case. (In both cases, the receiver was placed at the same latitude and longitude.) The difference of 2.8 km in source–receiver distance between the two cases can account for the 1.9-s travel time difference.

Figure 2 gives a projection of +35 ellipsoidal eigenray on the vertical source/receiver plane, and also a spherical ray path projection constructed using the same launch angle. The difference between the two paths represent the path error due to the neglecting of earth ellipticity. We can see from this figure that for the 1000-km path, the vertical difference due to earth flattening is small, and we did not observe significant horizontal deviations. However, Fig. 2 shows that the vertical path error due to earth flattening increased with ranges. Therefore, for longer transmissions, neglecting Earth flattening may produce large error in vertical paths.

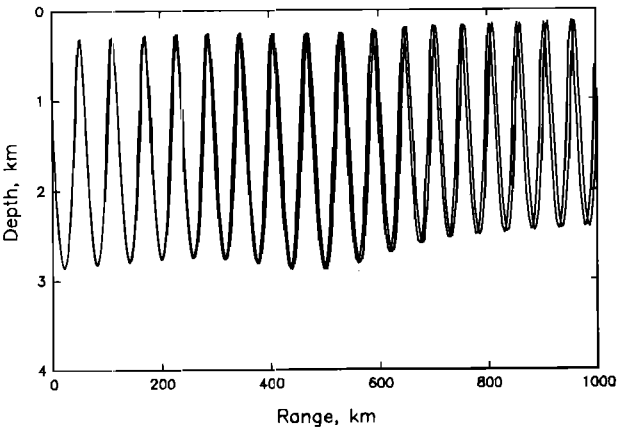

FIG. 2. Vertical difference in ray path due to Earth flattening. The path error increased with ranges.

Because of lacking sound speed data, we were unable to construct the Hawaii-to-California, and California-to-New Zealand paths which have been selected for use in the Acoustic Thermometry of Ocean Climate (ATOC) program. The ultimate success of ATOC depend, largely, upon the ability to solve forward problem accurately. Ellipsoidal ray equations can serve as a more accurate 3-D forward model.

ACKNOWLEDGMENTS

Part of this work was done at NOAA/Atlantic Oceanographic and Meteorological Laboratory while J. Yan held a Resident Research Associateship of the National Research Council. We thank the reviewer for many valuable comments in revising the manuscript. We are also grateful to Dr. T. M. Georges, Dr. W. J. Felton, and Dr. J. A. Mercer for familiarizing us with the 3-D sound speed model.

APPENDIX

To show that the second term and the last term of Eq. (46) vanish, we now show

$$\frac{\partial\sigma}{\partial\phi}+\frac{\partial\sigma}{\partial\dot{\lambda}}+\frac{\partial\sigma}{\partial r}=\frac{d}{ds}\left(\frac{\partial\sigma}{\partial\dot{\phi}}+\frac{\partial\sigma}{\partial\dot{\lambda}}+\frac{\partial\sigma}{\partial\dot{r}}\right). \tag{A1}$$

From Eq. (19), we write

$$\begin{aligned}\frac{\partial\sigma}{\partial\phi}+\frac{\partial\sigma}{\partial\dot{\lambda}}+\frac{\partial\sigma}{\partial r}=\dot{\phi}&\left[\mathbf{e}_\phi\left(\frac{\partial h_\phi}{\partial\phi}+\frac{\partial h_\phi}{\partial r}\right)+h_\phi\left(\frac{\partial\mathbf{e}_\phi}{\partial\phi}+\frac{\partial\mathbf{e}_\phi}{\partial r}\right)\right]\\&+\dot{\lambda}\left[\mathbf{e}_\lambda\left(\frac{\partial h_\lambda}{\partial\phi}+\frac{\partial h_\lambda}{\partial r}\right)+h_\lambda\frac{\partial\mathbf{e}_\lambda}{\partial r}\right]\\&+\dot{r}h_r\left(\frac{\partial\mathbf{e}_\mathbf{r}}{\partial\phi}+\frac{\partial\mathbf{e}_\mathbf{r}}{\partial\lambda}\right)\end{aligned} \tag{A2}$$

and

$$\frac{d}{ds}\left(\frac{\partial\sigma}{\partial\dot{\phi}}+\frac{\partial\sigma}{\partial\dot{\lambda}}+\frac{\partial\sigma}{\partial\dot{r}}\right)$$

$$=\dot{\phi}\left(\mathbf{e}_{\phi}\frac{\partial h_{\phi}}{\partial\phi}+h_{\phi}\frac{\partial\mathbf{e}_{\phi}}{\partial\phi}+\mathbf{e}_{\lambda}\frac{\partial h_{\lambda}}{\partial\phi}+h_{r}\frac{\partial\mathbf{e}_{\mathbf{r}}}{\partial\phi}\right)$$

$$+\dot{\lambda}\left(h_{\phi}\frac{\partial\mathbf{e}_{\phi}}{\partial\lambda}+h_{\lambda}\frac{\partial\mathbf{e}_{\lambda}}{\partial\lambda}+h_{r}\frac{\partial\mathbf{e}_{\mathbf{r}}}{\partial\lambda}\right)$$

$$+\dot{r}\left(\mathbf{e}_{\phi}\frac{\partial h_{\phi}}{\partial r}+\mathbf{e}_{\lambda}\frac{\partial h_{\lambda}}{\partial r}\right). \tag{A3}$$

Substituting Eqs. (A2) and (A3) into (A1) gives

$$(\dot{\phi}-\dot{\lambda})\left(h_{\phi}\frac{\partial\mathbf{e}_{\phi}}{\partial\lambda}-\mathbf{e}_{\lambda}\frac{\partial h_{\lambda}}{\partial\phi}\right)+(\dot{\phi}-\dot{r})\left(\mathbf{e}_{\phi}\frac{\partial h_{\phi}}{\partial r}-h_{r}\frac{\partial\mathbf{e}_{\mathbf{r}}}{\partial\phi}\right)$$

$$+(\dot{\lambda}-\dot{r})\left(\mathbf{e}_{\lambda}\frac{\partial h_{\lambda}}{\partial r}-h_{r}\frac{\partial\mathbf{e}_{\mathbf{r}}}{\partial\lambda}\right)=0. \tag{A4}$$

Using Eqs. (13)–(18), one can easily show that Eq. (A4) is satisfied. Therefore, the proof of (A1) is given.

[1] R. M. Jones, J. P. Riley, and T. M. Georges, "HARPO—A versatile three-dimensional Hamiltonian ray-tracing program for acoustic waves in an ocean with irregular bottom," NOAA Report, Environmental Research Laboratories, Boulder, CO (1986).

[2] T. M. Georges, R. M. Jones, and T. P. Riley, "Simulating ocean acoustic tomography measurements with Hamiltonian ray tracing," IEEE J. Ocean Eng. **OE-11**, 58–71 (1986).

[3] C. S. Chiu and A. J. Semtner, "A simulation study of cross-basin sound transmission from Heard Island to California," J. Acoust. Soc. Am. Suppl. 1 **88**, S92 (1990).

[4] C. S. Chiu, A. J. Semtner, C. M. Ort, J. H. Miller, and L. L. Ehret, "A ray variability analysis of sound transmission from Heard Island to California," J. Acoust. Soc. Am. **90**, 2331 (A) (1991).

[5] L. L. Ehret and C. S. Chiu, "Coupled-mode propagation through the transition zone between the Antarctic circumpolar current and the Pacific deep ocean," J. Acoust. Soc. Am. Suppl. 1 **88**, S93 (1990).

[6] D. F. Smith, L. L. Ehret, J. H. Miller, and C. S. Chiu, "Eigenray solution for cross-shelf propagation," J. Acoust. Soc. Am. Suppl. 1 **88**, S59 (1990).

[7] K. Aki and P. G. Richards, *Quantitative Seismology, Theory and Methods* (Freeman, New York, 1980), Vol. 2, pp. 724–725.

[8] W. H. Munk, W. C. O'Reilly, and J. L. Reid, "Australia–Bermuda sound transmission experiment (1960) revisited," J. Phys. Oceanogr. **18**, 1876–1898 (1988).

[9] C. E. Ewing and M. M. Mitchell, *Introduction to Geodesy* (American Elsevier, New York, 1970), pp. 9–17.

[10] K. D. Heaney, W. A. Kuperman, and B. E. McDonald, "Perth–Bermuda sound propagation (1960): Adiabatic mode interpretation," J. Acoust. Soc. Am. **90**, 2586–2594 (1991).

[11] J. G. Dworski and J. A. Mercer, "Hamiltonian 3-D ray tracing in the oceanic waveguide on the ellipsoidal Earth," Tech. Rep. Applied Physics Laboratory, University of Washington, APL-UM TR 8929, 19–20 (1990).

[12] G. Bomford, Geodesy (Oxford U.P., London, 1971), pp. 107–112, pp. 562–566.

[13] M. R. Spiegel, *Vector Analysis and an Introduction to Tensor Analysis* (McGraw-Hill, New York, 1959), 137 pp.

[14] C. A. Boyles, *Acoustic Waveguides: Applications to Oceanic Science* (Wiley, New York, 1984), 191 pp.

[15] W. A. Kuperman, "Three-dimensional ocean acoustic modeling," *European Conference on Underwater Acoustics*, edited by M. Weydert (Elsevier Applied Science, London, 1992), pp. 271–274.

[16] T. M. Georges, R. M. Jones, and J. P. Riley, "Simulating ocean acoustic tomography measurements with Hamiltonian ray tracing," IEEE J. Oceanic Eng. **OE-11**, 58–71 (1986).

[17] J. A. Mercer, W. J. Felton, and J. R. Booker, "Three-dimensional eigenrays through ocean mesoscale structure," J. Acoust. Soc. Am. **78**, 157–163 (1985).

[18] W. H. Munk, "Sound channel in an exponentially stratified ocean with applications to SOFAR," J. Acoust. Soc. Am. **55**, 220–226 (1974).

[19] W. J. Felton (private communication, 1993).

[20] W. H. Press, B. P. Flannery, S. A. Teukolsky, and W. T. Vetterling, *Numerical Recipes, The Art of Scientific Computing* (Cambridge U.P., New York, 1988), p. 554.